JOURNAL OF MATERIALS SCIENCE 20 (1985) 4431–4444

Barrier effects in dispersive media

ROBERT M. HILL, COLIN PICKUP
The Dielectrics Group, Chelsea College, University of London, Pulton Place, London SW6 5PR, UK

The effect of barrier layers with a generalized dielectric response on the measurement of the dielectric properties of materials are investigated, using the cluster model of relaxation to represent both the bulk and barrier properties. It is shown that the Maxwell–Wagner response is a limiting case and only applicable when the series elements are perfect, non-dispersive capacitors and resistors. A number of experimentally investigated systems are examined and it is shown that there is clear evidence for the proposed model in a wide range of applications.

1. Introduction

The measurement of the dielectric properties of a material requires the imposition of a pair of electrically conducting electrodes, usually on opposite faces of a thin parallel-sided slab of the material to be examined. Only in the particular case of semiconductor junctions can the electrodes be intrinsic to the sample for, in this case, the extrinsic highly doped p and n regions form the conducting electrodes to the low conductance space-charge junction region. There has been a continuing interest in the effect of electrode contacts (particularly contacts to semiconducting and semi-insulating materials) over many years, and although general observations of the effects of such contacts can be made, the exact nature of the contacted region and of the effects of charge build-up or depletion and of non-perfect charge exchange at the electrodes are, as yet, imperfectly understood. Recent advances in our understanding of the dielectric properties of semi-insulating and insulating materials [1, 2] has suggested the possibility of examining the macroscopic properties of surface layers by using the observed dielectric response of the sample with its electrodes. The aim here is to determine the types of response that can be expected, and to indicate where such effects have been observed experimentally. Where useful experimental data are available detailed analyses of the observed response in terms of bulk and surface layer properties will be made and discussed.

Conventially the bulk dielectric response of a sample can be measured in terms of the complex capacitance. When conductivity is present in the sample this gives a contribution which is in phase with the measuring a.c. voltage and hence contributes to the imaginary component of the capitance, the dielectric loss. Generally one particular process is of interest in the frequency range available and the capacitance can then be expressed as the sum of a dispersive component and the effective "infinite" frequency part which is totally real and, itself, given by the summation of the incremental capacitive dispersions which occur at higher frequencies than that of interest. Hence we have, with $i = \sqrt{-1}$,

$$C(\omega) = C'(\omega) - iC''(\omega) \quad (1a)$$

$$= \varepsilon_0 \frac{A}{d}[\varepsilon'(\omega) - i\varepsilon''(\omega)] - i\frac{\sigma}{\omega}\frac{A}{d} \quad (1b)$$

$$= \varepsilon_0 \frac{A}{d}[\chi'(\omega) + \varepsilon(\infty) - i\chi''(\omega)] - i\frac{\sigma}{\omega}\frac{A}{d} \quad (1c)$$

where ε_0 is the absolute permittivity, $8.85 \times 10^{-12}\,\mathrm{F\,m^{-1}}$; A is the area; d the sample thickness; $\varepsilon(\omega) - i\varepsilon''(\omega)$ is the frequency-dependent permittivity; $\varepsilon(\infty)$ the "infinite" frequency

0022–2461/85 $03.00 + .12

permittivity; $\chi(\omega) = \chi'(\omega) - i\chi''(\omega) = \varepsilon(\omega) - \varepsilon(\infty)$ the dielectric susceptibility; ω the measuring frequency in radians and σ the conductivity. The conductance of the sample G, the inverse of the resistance, is given by $\sigma A/d$ and hence the loss component of the capacitance, or the dielectric loss, is

$$C''(\omega) = \varepsilon_0 \frac{A}{d} \varepsilon''(\omega) + \frac{G}{\omega} \qquad (1d)$$

Electrically the three responses from the susceptibility, the "infinite" frequency permittivity and the conductance act as admittances ($Y = i\omega C$) in parallel and hence are directly additive, as in Equations 1a to c.

The simplest electrical model of a material on which electrodes have been superposed is to describe the bulk of the sample as having an electrical impedance Z_b, where $Z_b = 1/Y_b$, and the two regions in proximity to the electrodes as, jointly, having an equivalent impedance Z_s. As the bulk and surface regions are electrically in series the total impedance is the summation of these individual values, i.e. $Z_b + Z_s$. In general neither of the impedances will be either purely real or purely imaginary and it is an advantage of the dielectric technique of investigation, unlike for example conductivity measurement, that both components of the response can be observed. The capacitance of the series combination of the bulk and surface elements is given by

$$C(\omega) = (i\omega)^{-1}(Z_b + Z_s)^{-1} \qquad (2a)$$

$$= C_b(\omega)C_s(\omega)[C_b(\omega) + C_s(\omega)]^{-1} \qquad (2b)$$

In the particular case in which the impedance of the bulk is entirely real and that of the surface layer entirely imaginary, that is for the series combination of the bulk resistance R_b and the surface layer capacitance C_s, Equation 2b gives the well known Maxwell–Wagner [3, 4] response

$$C(\omega) = C_s(1 + i\omega R_b C_s)^{-1} \qquad (3a)$$

$$= C_s(1 - i\omega\tau)/(1 + i\omega^2\tau^2) \qquad (3b)$$

in which the characteristic relaxation time of the sample, τ, is given by the product $R_b C_s$. As can be seen by inspection of Equation 3b the Maxwell–Wagner response is of the Debye form [5]. Equation 3, however, contains three elements of information that are of direct use. At zero frequency the magnitude of the (totally real) capacitance is C_s, the surface layer value, and no d.c. current flows. The maximum in the loss component of the capacitance occurs at the radian frequency τ^{-1} ($= G_b/C_s$), and finally in the frequency range in excess of τ^{-1} the imaginary component tends asymptotically to the limiting value G_b/ω. Hence knowledge of any two of these three quantities allows complete evaluation of the system in terms of the postulated bulk and surface properties.

Unfortunately few real systems behave in this simple Maxwell–Wagner–Debye form. Indeed the observation of perfect Maxwell–Wagner behaviour in solids is doubtful, although it may be expected to be found in liquids which contain free ions. However it is just in the complexity of the experimentally observed behaviour that the information, which allows detailed evaluation of the system response, lies. In order to examine these more complex systems it is necessary to establish reasonable models for the actual behaviour of both the bulk and surface regions. To these can then be applied Equations 1 and 2 which will then characterize the broad features of the responses which might be expected. Once these have been established comparison with the experimental data can be made, both on qualitative and quantitative bases. In the following section the background to a comprehensive model of dielectric response will be suggested, and in Section 3 a range of computer-calculated model responses will be examined. In Section 4 a range of experimental observations will be analysed in terms of the model proposed in the preceding section, and finally the usefulness of the approach will be discussed.

2. Response model

2.1. Dispersive processes

Critical evaluation of the dielectric response of real materials has shown that the dielectric susceptibility can be expressed in the form [6, 7]

$$\chi(\omega) = \chi(0)F(\omega/\omega_x) \qquad (4)$$

where $\chi(0)$ is the magnitude of the susceptibility dispersion, i.e. the dielectric increment for the single process of relaxation, and $F(\omega/\omega_x)$ is the spectral shape function for this process normalized to the characteristic frequency ω_x. For bound dipolar charge centres the cluster model

of relaxation [8–10] has shown that the spectral shape function takes the form

$$F\left(\frac{\omega}{\omega_p}\right) = F_0^{-1}\left(1 + \frac{i\omega}{\omega_p}\right)^{n-1} {}_2F_1 \times \left(1 - n, 1 - m; 2 - n; \frac{1}{1 + i\omega/\omega_p}\right) \quad (5a)$$

where n and m, which have been determined as the correlation coefficients for specific intra-cluster and inter-cluster relaxation mechanisms, respectively, lie between zero and unity and F_0 is the normalizing parameter

$$F_0 = \Gamma(2 - n)\Gamma(m)/\Gamma(1 + m - n)$$

where $\Gamma(\,)$ being the gamma function and ${}_2F_1(,;;)$ the gaussian hypergeometric function. When the dipolar charges are only weakly bound to one another within the material, and particularly when they can only move effectively within limited dimensionality channels, as in the case of the quasi-free ions in fast ion conductors, the spectral shape function takes the form [11] for $1 < p + n < 2$

$$F\left(\frac{\omega}{\omega_p}\right) = F_0'^{-1}\left(1 + \frac{i\omega}{\omega_c}\right)^{n-1} {}_2F_1 \times \left(1 - n, 1 + p; 2 - n; \frac{1}{1 + i\omega/\omega_c}\right) \quad (5b)$$

in which p is the fractional correlation index for the transport of the quasi-free charge between clusters and F_0' is the equivalent normalizing constant

$$F_0' = \Gamma(2 - n)\Gamma(1 - p)\left(\frac{p + n - 1}{p\Gamma(2 - n - p)}\right)$$

Equations 5 contain, in their asymptotic behaviour at frequencies much greater and much less than the characteristic values ω_p and ω_c, respectively, the fractional power-law behaviour which has been found [1, 6, 7, 12, 13] to be the general feature of dielectric response in condensed matter. For the bound dipolar case

$$\chi(\omega) \propto \chi(0)(i\omega/\omega_p)^{n-1} \qquad \omega \gg \omega_p \quad (6a)$$

and

$$\chi(0) - \chi(\omega) \propto (i\omega/\omega_p)^m \qquad \omega \ll \omega_p \quad (6b)$$

whereas in the case of the quasi-free charges Equation 6a continues to apply, with ω_p replaced by ω_c, but the low-frequency behaviour now becomes

$$\chi(\omega) \propto (i\omega/\omega_c)^{-p} \qquad \omega \ll \omega_c \quad (6c)$$

The complex frequency terms in Equations 6 contain the well-established relationships between the real and imaginary parts of the susceptibility, initially reported by Jonscher [12] in the form

$$\chi''(\omega)/\chi'(\omega) = \cot(n\pi/2) \qquad \omega \gg \omega_p, \omega_c \quad (7a)$$

Equivalent relations can be determined from Equations 6b and c as

$$\frac{\chi''(\omega)}{\chi(0) - \chi'(\omega)} = \tan(m\pi/2) \qquad \omega \ll \omega_p \quad (7b)$$

and

$$\chi''(\omega)/\chi'(\omega) = \tan(p\pi/2) \qquad \omega \ll \omega_c \quad (7c)$$

respectively.

Making use of Equations 1, 4 and 5 the generalized dielectric capacitance of a sample can be expressed in terms of the effective complex capacitance and parallel conductance as

$$C(\omega) = S[\chi(0)F(\omega/\omega_x) + \varepsilon(\infty)] - iG/\omega \quad (8)$$

where S is the sample factor $\varepsilon_0 A/d$. The equivalent electrical circuit is shown in schematic form in Fig. 1. In this, and subsequent circuit representations, the non-Debye spectral dispersion $F(\omega/\omega_x)$ has been indicated by shading within the capacitor plates; single-line shading indicates the bound dipolar case of Equation 5a, cross-shading the quasi-free charge case of Equation 5b, and dot-shading the degenerate case in which only the high-frequency behaviour of Equation 6a has been seen experimentally. Discontinuous cross-shading, as in Fig. 1, is retained to indicate a non-specified dispersive element.

In order to make clear the difference between the bound dipolar case and the quasi-free charge case Fig. 2a shows the former response and Fig. 2b the latter. In each of these diagrams an "infinite" frequency capacitance, $S\varepsilon(\infty)$, has been indicated in the high-frequency region and a range of conductances in the low-frequency region. The large dispersions in both the real and imaginary parts of the capacitance in the quasi-free charge case, as the frequency tends to zero, can be clearly seen and it is also apparent that

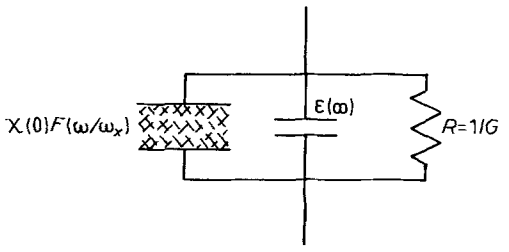

$$C(\omega) = S[\{\chi(0)F(\omega/\omega_x) + \varepsilon(\infty)\} - iG/\omega]$$

Figure 1 A generalized circuit element that has been constructed from a dispersive susceptibility, $\chi(0)F(\omega/\omega_x)$, a non-dispersive capacitance of permittivity $\varepsilon(\infty)$, and a conductance of magnitude G. S is the sample factor $\varepsilon_0 A/d$ and ω the frequency.

there is a minimum value of the conductance that can be differentiated from the loss dispersion in this case.

2.2. Electrode/surface characterization

Two broad patterns of behaviour can be used to characterize the surface layers adjacent to the electrodes. A Schottky-like depletion region can be envisaged in which a high-resistance layer of thickness d_s is established on balancing the contact potential differences between the electrodes and the bulk and on filling surface states where these exist. In this case one might be reasonably correct in modelling the surface layer as a capacitance of large magnitude. Alternatively a pool of charge could be injected into the sample from the electrode, in which case the pertinent characterization parameter might well be the surface layer conductance. The complex capacitance contained in Equation 8, however, has both these forms as limiting cases and it is obviously convenient, apart from retaining generality, if the response of the surface layer is taken as being qualitatively similar to that already attributed to the bulk of the material. By doing so the quantitative differences between the bulk and surface regions can be determined from the magnitude of the parameters deduced from analysis of the experimental data without constraints being imposed on the system. This approach has the additional advantage of retaining the elements of the cluster model of dielectric relaxation within both surface and bulk regions and, in particular, it allows estimation of the nature of correlation effects within both regions to be evaluated.

2.3. Diffusion barrier layers

Examination of a range of experimental data has shown that in a number of cases which are of interest the lowest-frequency dielectric response can be characterized by Equation 6a with n taking a value close to 1/2. It has already been pointed out [11, 14] that this type of response can be expected when a charge barrier layer is formed by diffusion. The more general case will be considered here in which

$$\chi(\omega) = \chi(\omega_d)(i\omega/\omega_d)^{-s} \quad s \sim 0.5 \qquad (9)$$

defines a barrier-layer susceptibility of magnitude

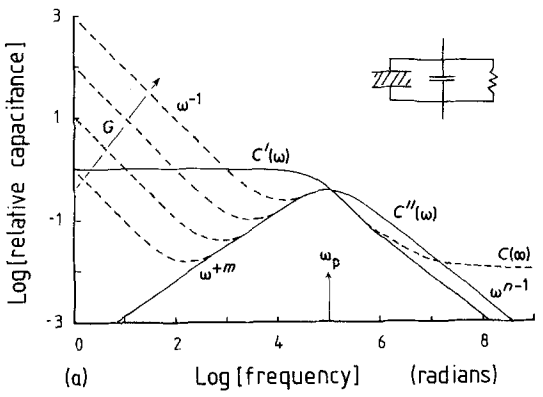

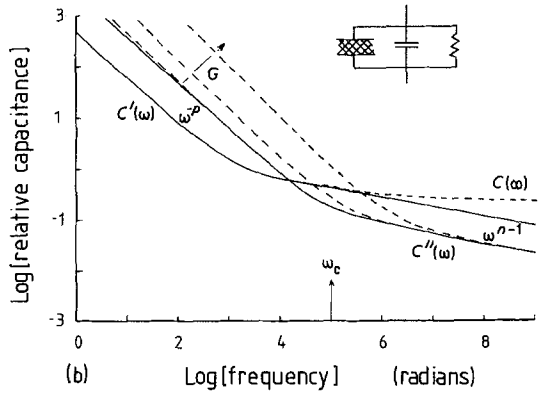

Figure 2 Schematic frequency response for the bound-charge, loss-peak and quasi-free charge, anomalous-dispersion processes. In both cases the effect of parallel conductances, of magnitude G, and an "infinite" frequency, non-dispersive capacitance $C(\infty)$ are shown by dashed curves. The plots are in relative units. (a) The bound charge behaviour with $m = 0.7$, $n = 0.2$ and $\chi(0) = 1.0$. The characteristic frequency ω_p is indicated, the conductances range from 1.0 to 10^3 and the "infinite" frequency capacitance is of magnitude 0.1. (b) the quasi-free charge-dispersion behaviour with $p = 0.9$, $n = 0.8$ and magnitude 1.0. The characteristic frequency is indicated as ω_c, the conductances range from 10^4 to 10^6 and $C(\infty)$ is 0.3.

$\chi(\omega_d)$ at a frequency ω_d which lies within the measured range of fractional power-law response. This form of definition has to be used as there is no characteristic frequency experimentally accessible. The barrier element defined by Equation 9 has the unusual property that it interacts with either a series resistance or a series capacitance to give dispersions which are not of simple, single power-law form.

The series resistance case has already been considered by Jonscher [1]. Letting the capacitance of the diffusive barrier layer be given by

$$C_d(i\omega/\omega_d)^{-s} \tag{10}$$

where $C_d = S\chi(\omega_d)$, and letting the series resistance be R, the resultant capacitance of the system is

$$C(\omega) = \frac{C_d^2 R(iz)^{-s}[1 - (iz)^{1-s}RC_d]}{1 + z^{2-2s}R^2C_d^2 + 2z^{1-s}RC_d \sin(s\pi/2)} \tag{11}$$

where $z = \omega/\omega_d$. In the limiting case of low frequencies the fractional power-law behaviour of Equation 10 is recovered, whereas at high frequencies the imaginary component is $(\omega R)^{-1}$ with the real component becoming

$$C'(\omega) = R^{-2}C_d^{-1}z^{s-2}\cos(s\pi/2) \tag{12}$$

as indicated in Fig. 3a.

Taking the same capacitative barrier in series with a non-dispersive capacitance of magnitude C gives the equivalent response as

$$C(\omega) = \frac{CC_d[C(iz)^{-s} + C_d z^{-2s}]}{C^2 + C_d^2 z^{-2s} + 2CC_d z^{-s}} \tag{13}$$

which gives a peak in the loss component at the frequency ω_s where

$$\omega_s = \omega_d(C_d/C)^{1/s} \tag{14}$$

and the loss curve is symmetrical about ω_s, that is the characteristic of Equation 13 is of the Cole–Cole [15] form with the Cole–Cole parameter β given by $(1 - s)$. Fig. 3b shows that the complete response is dominated by the capacitance C at low frequencies ($C_d(i\omega)^{-s} > C$), and that ω_s is the frequency at which the magnitudes of the two elements are equal.

2.4. Series combination

In the previous subsection the series response of the diffusive barrier and the single perfectly resistive or capacitative elements have been examined. In the more general case, indicated in Fig. 4, analytical evaluation is no longer simple and recourse has to be made to computer modelling. Because of the power-law behaviour that is present in the responses it has been found convenient to use log–log plots for the frequency response of the capacitance. As indicated briefly in Section 1, the responses could equally well be represented in terms of admittance or impedance. The quasi-free carrier response has commonly been presented in terms of the dielectric modulus, the inverse of the capacitance or permittivity, for in this representation the modulus tends to zero at zero frequency. Each of these presentations has its advantages and disadvantages, but all are essentially equivalent. Other techniques of presentation have been used, the most common of which is the Cole–Cole plot [15] in which the imaginary part of the response is plotted as a function of the real part using linear scales. For the perfect Debye case of Equation 3b a semicircle is obtained, and hence this is a convenient technique for testing the degree of fit to the

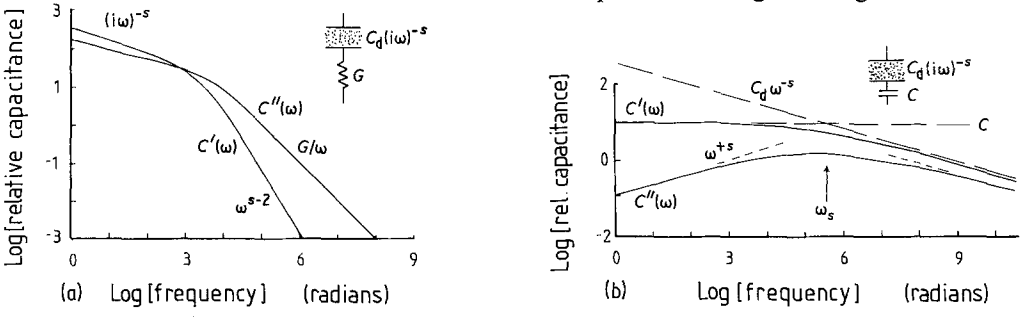

Figure 3 The response characteristics of a diffusive boundary layer in series with (a) a conductance and (b) a capacitance. In both cases the diffusive capacitance is of magnitude 3×10^2 relative units at one radian and $s = 0.3$. The conductance value is 10^{-5} and the capacitance 10. Note the ω^{s-2} asymptotic behaviour in the real part of the capacitance at high frequencies.

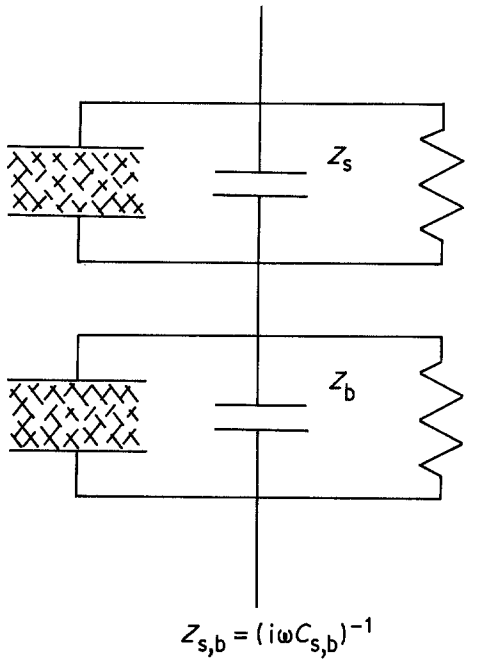

Figure 4 The series arrangement of two elements of the type shown in Fig. 1. Arbitrarily one element has been associated with the bulk material response and is of impedance Z_b, whilst the other element is associated with the surface-layer response and has impedance Z_s.

Debye characteristic. With fractional power-law response the Cole–Cole plot gives lines of constant gradient at the high and low frequency limits (see Equations 7) but the common lack of accessible frequency information on these plots is a disadvantage as Jonscher [1, 16] has indicated in his examination of these alternative methods of presentation.

One criticism of computer-fitting the observed responses by a series pair of elements is the large number of free variables that are present. In practice good fitting can only be achieved when there is sufficient information in the reported experimental data to characterize all the *necessary* parameters. It has been the practice here to always use the *minimum* number of circuit elements that are essential for a fit to the experimental data.

3. Computed responses

Before analysing specific experimental data a number of model characteristics will be presented in this section, in order that the broad features of the experimental results in the following section may be understood. Fig. 5 shows the response for a conventional series pair of parallel, non-dispersive resistance and capacitance combinations. The curves shown in Fig. 5a have been obtained by using the values of R and C listed in the caption. These values have been chosen so that one parallel pair dominate the response at high frequencies and the other at low frequencies. The structure in this plot can be understood in terms of the transfer of the effective impedance within the complete system from one element of the series pair to the other as the frequency is varied. The comparable response shown in Fig. 5b has been obtained

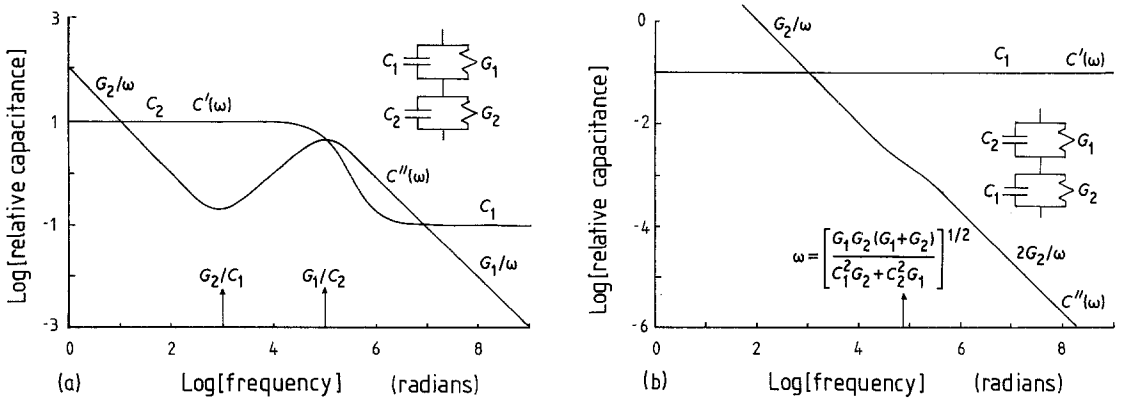

Figure 5 The response of a series combination of G and C parallel elements. In both cases $C_1 = 0.1$, $C_2 = 10$, $G_1 = 10^6$ and $G_2 = 10^2$, in relative units. The characteristic shown in (a) indicates the dominance of the combination G_1 and C_1 at high frequencies and the combination G_2 and C_2 at low frequencies. Plot (b) has been obtained by interchanging the capacitative elements and is dominated throughout the frequency range by the parallel combination of G_2 and C_1. In (a) the inverses of the relaxation times are indicated and the Maxwell–Wagner–Debye characteristic in the region of (G_1/C_2) is clearly shown. In (b) the slight change in magnitude of the loss component in the region 10^5 radians is due to the presence of the second element, and is the only indication of it. The calculated inflection frequency is shown.

using the identical circuit components but exchanging the two capacitances. In this case the dominant behaviour is that of the higher impedance element throughout the frequency range and there is only a weak indication, by an increase in the loss component by a factor ($2^{1/2}$ for the R and C values used here), of the lower impedance element which is in series with it. This dominance by one element clearly shows how, in many dielectric investigations, the effect of the putative surface layers is not observed; their impedance is sufficiently smaller than that of the bulk so as not to contribute significantly to the response.

As discussed earlier Fig. 5a contains sufficient information to allow complete analysis of the magnitudes of the individual components of the original circuit. In particular it should be noted that the conductance elements transform, in this log–log plot, into segments of straight lines of gradient (-1) for the imaginary component of the complex capacitance. This is a basic feature of these plots and it will be used not only as a strong indicator of the existence of conductance (resistance) elements but also of their magnitude.

The spectral response of a diffusive barrier layer in series with a parallel G and C combination is shown in Fig. 6a. The observed response is a compound of that already presented in Fig. 3, with both the quasi-Debye dispersion due to the series resistance and the Cole–Cole dispersion due to the series capacitance being evident. With the particular value of s used here, 0.3, a wide frequency range has been required to cover the full characteristic. The following diagram (Fig. 6b) indicates how the high-frequency Cole–Cole dispersion can be removed by the presence of a second capacitive element in parallel with the diffusive boundary element. Physically this occurs when there is a minimum distance over which diffusion can take place. The magnitude of this parallel capacitance is shown in the diagram as $C_2(\infty)$, but any value lying between this and $C_1(\infty)$ is sufficient to saturate the barrier-layer capacitance and remove the high-frequency Cole–Cole dispersion.

The almost d.c. properties of the loss component of the quasi-free charge case can act in a similar manner to a conductance. Fig. 6c shows the comparable response to that of Fig. 6a with

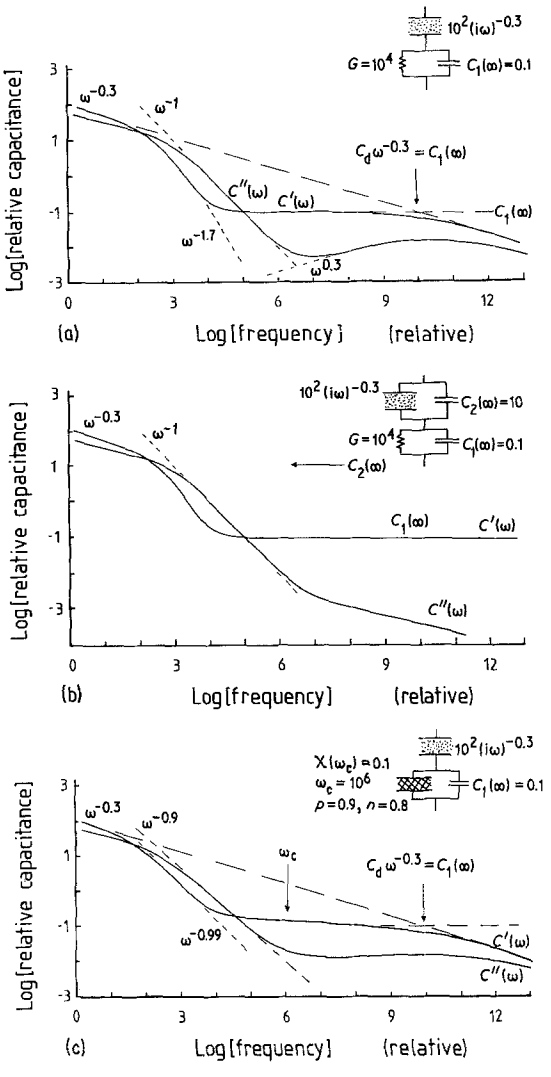

Figure 6 (a) The dispersion from a series combination of the diffusive element of Fig. 3 and a G and C parallel combination. The response contains both the forms presented in Fig. 3 in parallel summation. (b) With a suitable capacitance in parallel across the diffusive barrier element the condition for the high-frequency Cole–Cole type of dispersion in (a) is invalidated and this loss peak does not develop. (c) On replacing the conductive element with a quasi-free charge dispersion process a further generalization of the Maxwell–Wagner response has been obtained. In this case the gradient of the loss in the Maxwell–Wagner dispersion region is $(-p)$ in place of (-1) and there is a further reduction in the magnitude of the gradient in the real component. The high-frequency loss peak response continues to be present in the absence of a blocking capacitor in parallel with the diffusive barrier layer.

the conductance replaced by an almost equivalent quasi-free charge element. The same broad pattern of behaviour can be seen and the high-frequency Cole–Cole type of dispersion

can, again, be eliminated by having a suitable capacitance in parallel with the diffusive barrier element. The essential difference between the plots shown in Figs. 6a and c is in the gradients of the loss and capacitance in the frequency range between 10^2 and 10^4 frequency units. Essentially Fig. 6c presents a generalized Maxwell–Wagner response, and that contained in Fig. 3a is the particular limiting case when transport is non-dispersive.

4. Experimental responses

A range of experimentally determined dielectric responses will be examined and analysed in this section in terms of the model derived in Section 2. The common feature in the choice of data was the presence of barrier-layer effects in series with a bulk dielectric response. In the first case that will be considered the barrier has been introduced artificially, whilst in all the other cases the barrier/surface layers are intrinsic to the samples or to their method of preparation.

4.1. Blocking contact to GaAs

Fig. 7a shows the dielectric response measured on a sample of gallium arsenide. The "infinite" frequency capacitance, 2.9×10^{-11} F, agrees with the sample factor and the quoted bulk dielectric constant of 12.95. For frequencies less than 10^3 Hz there is a dispersion in the real part of the capacitance, of magnitude 7.8×10^{-10} F, which can be associated with the formation of a Schottky surface layer. The parallel conductance can be determined from the low-frequency loss as $3.2 \times 10^{-9}\,\Omega^{-1}$. The curves through the data points in Fig. 7a were obtained using these values and spectral shape parameters of $n = 0.5$ and $m = 0.6$. The data shown in this figure were measured at 295 K and evaporated aluminium electrodes were used, contact to the electrodes being made by copper wires and conducting silver paste. The equivalent response shown in Fig. 7b was obtained from the same sample, at 300 K, but with contacts of thin aluminized polymer foil held between the aluminized sample faces and pressure pads. The series capacitance of the foils was 3×10^{-10} F and they were of low loss. The plots through the data points in Fig. 7b were obtained by inserting this value of capacitance in series with the element parameters obtained from the previous curve fitting. As can be seen, good agreement has been obtained with the experimental data. The only feature shown in this figure that is not reproduced by the model structure is the loss response in the region of 10^{-2} Hz, which is due to the loss in the polymer foil and is not sufficiently resolved to be introduced into the model.

Examination of the magnitudes of the responses in Figs. 7a and b shows that not only have the blocking contacts eliminated the d.c. conductance but they have also affected the magnitude of the dispersion. The series model, however, automatically takes this into account. For perfect blocking with no dispersion

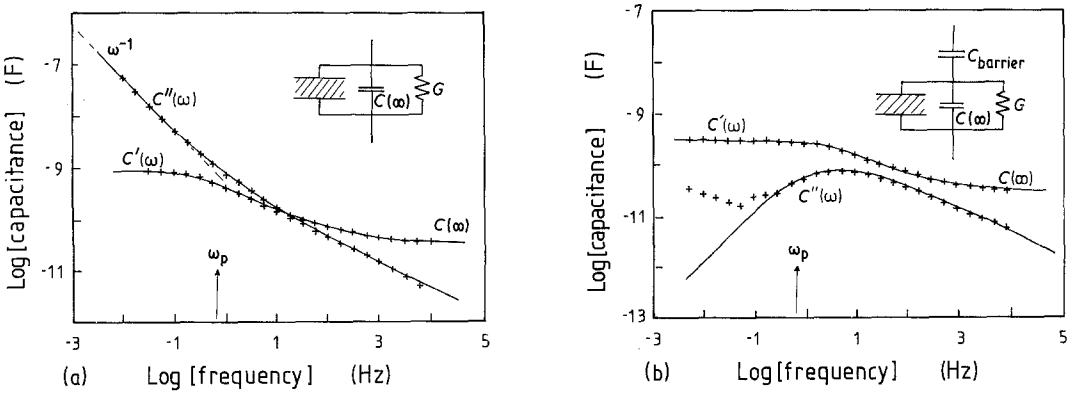

Figure 7 The dielectric response of a sample of gallium arsenide with non-blocking and blocking surface layers. (a) Non-blocking contacts. The plots through the data points have been obtained by making use of the circuit shown in the inset, with $C(0) = 7.8 \times 10^{-10}$ F, $m = 0.6$, $n = 0.5$, $\omega_p = 6.1 \times 10^{-1}$ Hz, $C(\infty) = 2.9 \times 10^{-11}$ F and $G = 4.5 \times 10^{-9}$ S. (b) Blocking contacts. The data points show the response for the same sample on using thin aluminized polymer foil as the electrodes. The total capacitance of the foils was 3.0×10^{-10} F and the curves through the data points have been obtained by using this value of capacitance in series with the circuit elements characterized in (a).

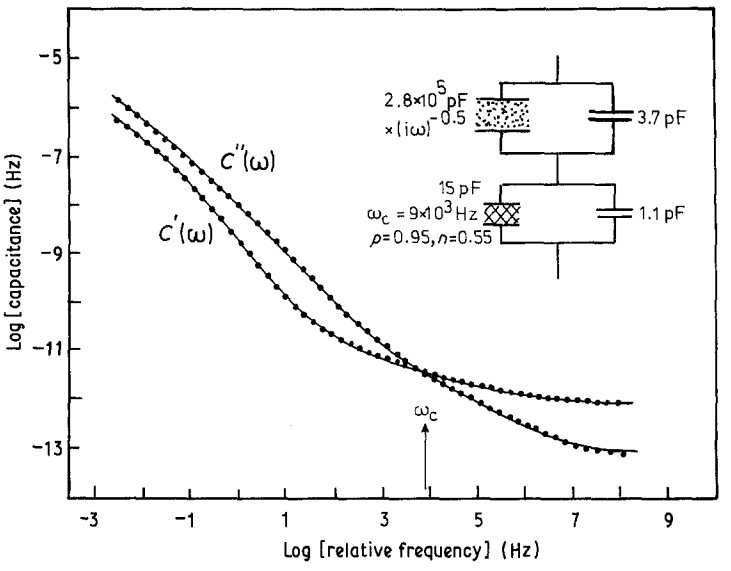

Figure 8 The dielectric response of a porous ceramic catalyst containing adsorbed water as reported by Ramdeen *et al.* [17]. The magnitudes of the circuit elements used in curve-fitting the data points are given in the insert. The presence of the capacitance in parallel with the diffusive element is required by the form of the high-frequency response of the loss component. The square-root asymptotic dependence at low frequencies is approached but not reached in this temperature-normalized plot.

distortion a larger series capacitance would be required.

4.2. Catalyst in a humid atmosphere

As the second example the dielectric properties of a sample of porous ceramic catalyst with evaporated aluminium electrodes will be examined. When this highly porous material is held under high-humidity conditions water molecules adsorb on to the internal pore surfaces. At very high humidities the d.c. conductance can be found, although a more common response is the dispersion due to a quasi-free charge transport [17]. In the temperature range from room temperature to 373 K the characteristic shown in Fig. 8 was obtained by temperature-normalizing the measured data (Fig. 3b) of Ramdeen *et al.* [17]. The general form here is of the type already indicated in Fig. 6, in which a barrier layer with fractional power-law behaviour is in series with the quasi-free charge dispersion process characteristic of the bulk response. The curves through the data points in this figure have been obtained by using the circuit elements shown in the inset to the figure with the values indicated. A true diffusive barrier has been formed in this material, $s = 0.5$, but even the extended normalized frequency does not go low enough to show the equality of the real and imaginary components (Equation 7a). The weak interaction between the extrapolation of the $\omega^{-1/2}$ characteristic and the high-frequency loss indicates that the conditions of Fig. 6b apply with a small capacitative element in parallel with the diffusive barrier layer. The large value of p, 0.97, indicates that the ion motion in the water adsorbate is highly correlated and approximates closely to a d.c. conduction process. As the response is sensitive to the amount of water adsorbed [17] it has been proposed that the mobile ions are hydroxyl ions. The large dispersion caused by the formation of the diffusion barrier indicates that it has a thickness of about 10^{-6} of the total sample thickness, that is in the region of 3 nm when fully developed at the lowest relative frequencies.

4.3. Semiconducting aggregate

The dielectric response, in terms of relative permittivity, of a sintered semiconducting aggregate of $MgAl_{0.4}Fe_{1.6}O_4$ with evaporated silver electrodes is shown in Fig. 9a. The data were measured over the temperature range 227 to 344 K by Fairweather and Frost [18] and the diagram presents the data in a temperature-normalized form [6] with the plot scaled for 344 K. The permittivity is scaled in terms of the high-frequency value at this temperature which was quoted by Fairweather and Frost as 17. The curves through the data have been obtained by modelling the response as a quasi-free carrier element in series with a parallel conductance and capacitance combination. The inset to the figure gives both the circuit diagram and the values of the individual parameters. Physically the material was reported as being formed of local crystalline particles with the interstices between these filled with poorly ordered resistive semi-

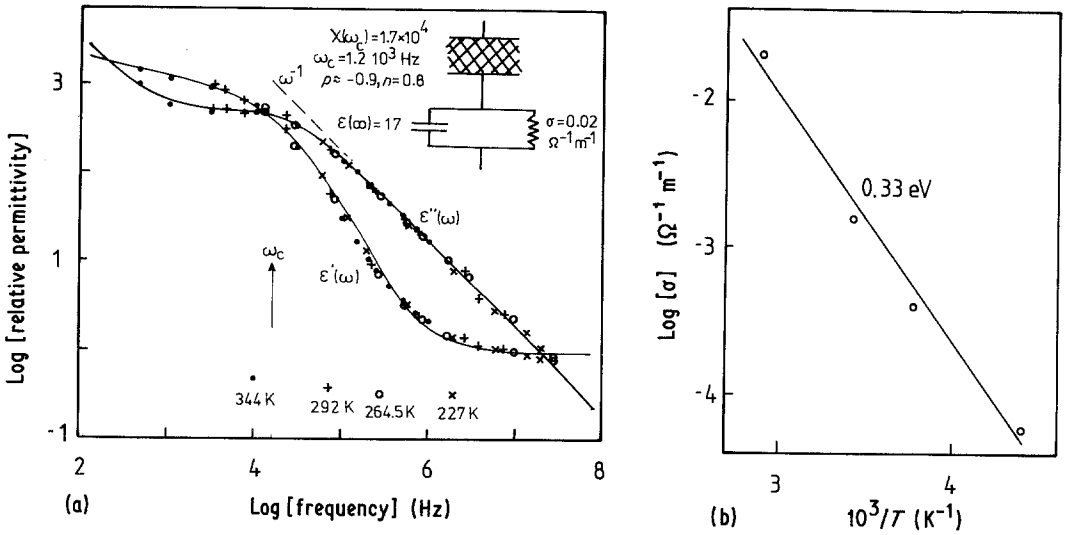

Figure 9 The dispersion in permittivity reported by Fairweather and Frost [18] for an aggregated sample of the semiconductor $MgAl_{0.4}Fe_{1.6}O_4$. The principal feature here is the modified Maxwell–Wagner response of the type shown in Fig. 6a. The frequency range is too limited at high frequencies to indicate whether a second capacitative element is in parallel with the quasi-free charge dispersion element. The anomalous low-frequency dispersion of Equation 6c is also poorly characterized and the value of p, 0.9, can only be taken as approximate. (a) The temperature-normalized characteristic scaled at 344 K and fitted by the circuit shown in the inset. (b) An Arrhenius plot of the temperature dependence of the conductivity as indicated by the relative frequency shift of a temperature datum point, 10^4 Hz and 0.5 permittivity, showing that the conductivity is activated with an energy of 0.33 eV.

conductor. In the original analysis of the data [18] the dielectric response was modelled by a three-element R–C circuit, using non-dispersive R and C elements. The agreement between the measured response and that determined from the model was relatively poor. The essential difference between that construct and the one presented here is the recognition that the lowest frequency response is caused by a quasi-free carrier dispersion. The large magnitude of this response indicates that the quasi-conduction region can be associated with the thin layer of interparticulate material, the individual particles exhibiting a strong conductivity in parallel with a high permittivity, typical of an ordered semiconductor.

We expect ω_c and $\chi(\omega_c)$ to be temperature-dependent, but the principal temperature dependence seen in this normalized plot is that of the conductivity, for only the highest-temperature data give information in the region of ω_c. Fig. 9b presents an Arrhenius plot for this conductivity which can be seen to be activated with an activation energy of 0.33 eV. In the ordered particles the carriers will be either electrons or holes which become blocked in the interparticle disordered regions. It is likely that the same carriers contribute to the quasi-free carrier transport.

4.4. Ion-exchange resin

The response from a qualitatively similar but quantitatively different model structure is shown in Fig. 10. The data presented here were measured by Ishakawa *et al.* [19] for the response of an ion-exchange resin in water using platinum electrodes. The resin was a sodium-form SP-Sephadex C–25 and the sample was measured at 297 K. Here there is no doubt about the quasi-free carrier dispersion process, the low-frequency parallel dispersions in the real and imaginary parts of the capacitance being particularly well developed. The conductivity acts as a high-frequency cut-off giving the generalized Maxwell–Wagner response characteristic in the region of 10^7 to 10^8 Hz. There is also no doubt that in this case the transport is due to ion motion in water ($\varepsilon = 86$) and the formation of electrical double layers around the resin particles at low frequencies leads to the quasi-free charge process which decreases the effective transport. At 10^5 Hz the ratio of the extrapolated d.c. conduction to the magnitude of the loss component of the quasi-free charge

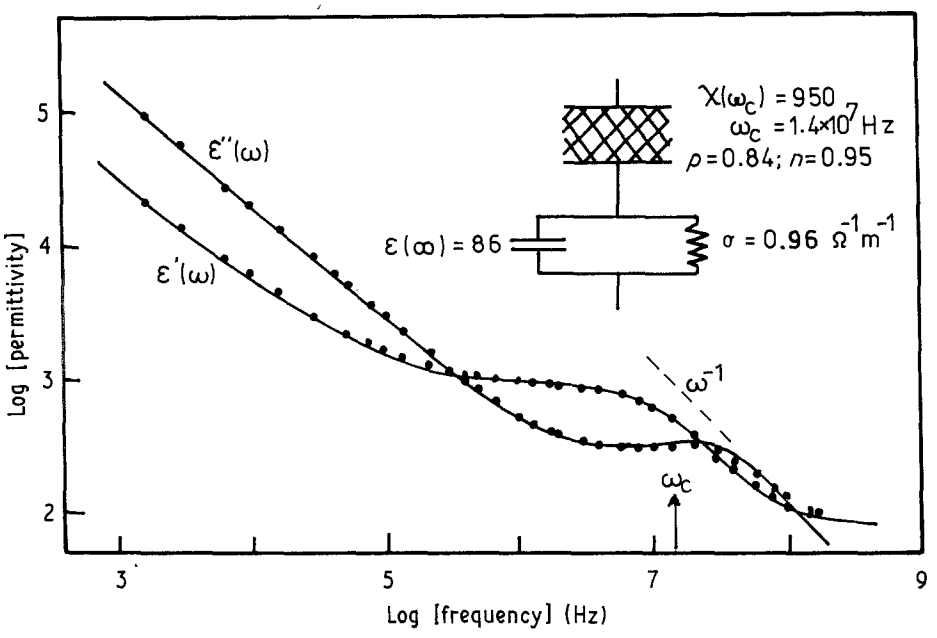

Figure 10 The dielectric response of an ion-exchange resin in water. The data are taken from Ishikawa *et al.* [19]. Qualitatively this characteristic is comparable to that shown in Fig. 9 but the relatively higher conductivity has allowed the development of the quasi-free charge low-frequency dispersion. In this case the inset shows that the entire response has been modelled using only three circuit elements, each of which is well characterized.

dispersion is about 30 : 1, indicating a transport efficiency of about 3%.

There is no evidence in the experimental data for diffusion taking any part in the formation of the double layer, nor is there any evidence for a frequency-independent capacitance in parallel with the quasi-free charge dispersion. Hence at high frequencies, in excess of 10^8 Hz, the system would act as a conductivity and permittivity in parallel. At lower frequencies an almost frequency-independent boundary layer is formed ($1 - n = 0.05$) to give the almost perfect Maxwell–Wagner response which blocks the conductivity, and which, in turn, exhibits the limited transport of the quasi-free charge dispersion.

4.5. Electrolytic cell

As a final example the frequency response of the measured capacitance of one electrode in an electrolytic cell is shown in Fig. 11. The data were obtained by Briggs [20] by using a three-terminal technique in which a reference electrode probe was placed in the 1 M aqueous H_2SO_4 solution about 5 mm away from the surface of the 0.36 cm^2 platinum electrode surface. The measurements were made at 298 K and a fixed d.c. bias between the platinum and reference electrode corresponding to the onset of the hydrogen evolution reaction at the platinum electrode surface. The d.c. cell current, measured both before and after the frequency run, was 5 μA $\pm$ 50%, and the response was linear in a.c. field for the small test potential of 5 mV rms which was used.

The data have been fitted over the measured range of 10^{-1} to 10^4 Hz by the circuit shown diagramatically in the inset to Fig. 11. The series conductance here is the purely real impedance of the electrolyte, and the Helmholtz double layer at the surface of the platinum has been modelled by a diffusive element of magnitude 1.1×10^{-2} F (at 1 radian) in parallel with a conductance of 2.33×10^{-2} S and a non-dispersive capacitance of magnitude 1.2×10^{-4} F. The non-dispersive capacitance again implies that there is a minimum path length over which diffusion can take place. Taking a relative dielectric constant of 80 for the solution the minimum path length can be estimated as 0.21 nm, that is of the order of an atomic spacing. The particles taking part in the diffusion process are charged and hence contribute an a.c. current to the total current flow. At a frequency of one radian the fraction of the total charge carried by diffusion is 0.32. The

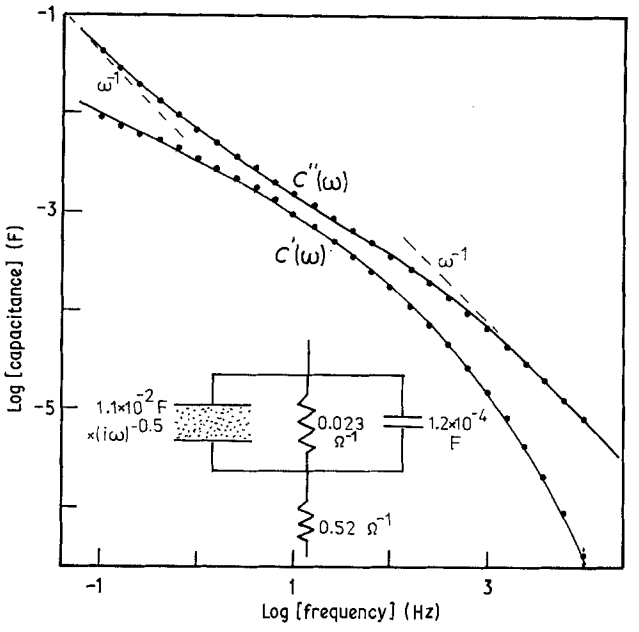

Figure 11 The dielectric response of the electrode region of an electrolytic cell. A three-terminal probe technique was used and the cell was biased to the onset of hydrogen evolution at the platinum electrode. The experimental data were communicated by Briggs [20]. The series conductance is that of the 1 M H_2SO_4 electrolyte, and the triple-component element in series with it models the response of the Helmholtz double layer at the electrode.

minimum diffusion path length is reached for frequencies in excess of 1.3×10^3 Hz and in this frequency region the system behaviour is a conventional Maxwell–Wagner response with the solution conductance in series with the fixed monolayer capacitance at the electrode and its parallel but small leakage conductance.

5. Discussion

A range of solid and liquid barrier systems have been examined and it has been shown that the experimental data can be reproduced accurately using the series circuit shown diagrammatically in Fig. 4. In general it has been found that only four of the six possible elements have been required, but in all cases the dispersive capacitative element defined by Equations 4, 5 and 9 has been found to be an essential feature of the response. Non-dispersive resistance and capacitance-element circuit modelling has been extensively used [21], but this results in complicated many-element networks which may have limited applicability, and which do not reveal the basic physics of the elemental responders. The observation of dispersive elements in bulk dielectric response is well established [1, 6, 7] and here it has been shown they are also present in barrier layers. The particular case of the diffusive element, defined by Equation 10 with $s = 1/2$, has been modelled by Warburg [14] as an infinite chain of resistors and capacitors, whereas in terms of the cluster-model approach the characteristic develops naturally from the $t^{-1/2}$ time-dependence of classical diffusion.

It is not our intention here to discuss the physics of the dispersive elements for each of the cases examined. To do so would require more experimental data than have been reported. Such discussions have already been given, for both bound-charge cases [22–25] and for a quasi-free charge carrier case [17]. We will, however, examine the differences between the three types of dispersive element which have been observed. In the gallium arsenide sample Fig. 7a shows the development of a Schottky barrier at low frequencies. Modulation of the barrier by the a.c. probe voltage sweeps charge in and out of the barrier as it grows and contracts, hence, this charge is essentially bound. The charge that is transported across the barrier forms a parallel leakage current. The values for the spectral shape or correlation parameters, $m = 0.6$ and $n = 0.5$, indicate that the charge movement is diffusion-like. In our experience these m and n values are typical for Schottky barriers over a range of semiconductors. The relaxation time for the barrier formation, 0.26 sec, is, in the cluster model, the relaxation time averaged over all the elemental cluster responses which form the Schottky response. Hence this time is to be associated with the barrier formation and not with the individual relaxation times of excitation or recombination of charges.

The quasi-free carrier response, in which the transport of charge is imperfect, has been observed in the wet porous ceramic, in the barrier layers between the semiconducting aggregated particles, and in the ion-exchange resin. In the first of these it has been shown [17] that this quasi-d.c. transport is through the water adsorbate within the channels in the ceramic, and the particular feature of interest here is the observation of diffusive behaviour at low frequencies, which even further limits charge transport, and which is almost certainly due to charge build-up in the region of the electrodes. The observation of the quasi-free carrier transport in the sintered semiconductor is unexpected and must be related to charge build-up on the surfaces of the conducting particles. If the disordered material between the particles is not stoichiometric then it is possible that ion motion occurs at least over limited path lengths. We note that the characterization of the highly dispersive regions is very poor and that we have little real information about the magnitude of p. On the evidence that exists there is no leakage current in parallel with the quasi-free charge dispersion. If we assume, as is likely to be the case, that the current within the particles is electronic and the charge transport between the particles is ionic, then the transport is limited either by inefficient charge exchange at the surfaces of the particles or by the limited supply of quasi-free ions. The quasi-free charge transport could then be envisaged as the imperfect transmission of locally induced ionic displacements throughout the system. In contrast the ion-exchange resin system gives an almost perfect quasi-free charge dispersion. At high frequencies (where the a.c. path length is small) there is a conductivity in parallel with the solvent permittivity, but at low frequencies (where the path length is longer) the transport is no longer coherent. This is reflected in the magnitudes of the correlation coefficients n and p. The former, the local correlation index, is high at 0.95, whereas the latter, the long-range inter-cluster index, is lower at 0.84, and can be taken as a direct measure of the perfection of long-range transmission of charge displacements in the system.

Perfect classical diffusion $s = 0.5$, has been observed in two cases: in the barrier layer to the wet ceramic and in the Helmholtz layer at the platinum electrode in the electrolytic cell. Neither of these results is unexpected. In both cases there are minimal path lengths for the onset of diffusion, which in the case of the electrolytic cell is about a monolayer in thickness but in the ceramic sample is about one-third of the sample thickness. These reflect the differences between the two systems. In the former, charge transport in a coherent, conductive, manner occurs in the bulk of the material. Only at the electrodes is a space-charge established and charge exchange takes place by diffusion through this surface layer. The surface layer only exists when sufficient charge per half-cycle reaches the electrode. In contrast the diffusional transport is always present for the water adsorbate in the porous ceramic. At sufficiently high frequencies ($\omega > \omega_c$) the latent diffusional charges have a sufficiently small path length that they remain correlated with their countercharges. Classical diffusion requires no correlation and hence can only occur once inter-cluster exchange processes have separated the charge and its countercharge.

6. Conclusions

It has been established that the description of the dielectric response of barrier effects requires the use of dispersive elements. It has been further shown that the Dissado–Hill cluster model of relaxation is a suitable basis for the detailed description of these dispersive elements. Barrier effects have been investigated in a wide range of dielectrically active systems comprising crystalline and disordered semiconductors, a porous ceramic under humid atmosphere conditions, an ion-exchange resin in water, and an electrolytic cell. As a result a range of bulk- and barrier-types of response have been observed and modelled satisfactorily. It is realized that any series circuit can be represented as an electrically equivalent parallel circuit, but here we have chosen the simplest form of circuit in each case and have been guided in this choice by the physics of the systems that have been investigated.

Acknowledgements

The authors gratefully acknowledge the assistance of Mr A. Briggs, who kindly supplied data on the electrolytic cell response prior to publication, and of Dr L. A. Dissado who critically read the manuscript.

References

1. A. K. JONSCHER, "Dielectric Relaxation in Solids" (Chelsea Dielectrics Press, London, 1983) p. 93.
2. R. M. HILL, *Thin Solid Films* **125** (1985) in press.
3. J. C. MAXWELL, "Treatise on Electricity and Magnetism", 3rd Edn (Dover, New York, 1954).
4. R. J. WAGNER, *Ann. Physik* **40** (1913) 317.
5. P. DEBYE, "Polar Molecules" (Dover, New York, 1945).
6. R. M. HILL, *Nature* **275** (1978) 96.
7. *Idem, J. Mater. Sci.* **16** (1981) 118.
8. L. A. DISSADO and R. M. HILL, *Nature* **279** (1979) 685.
9. L. A. DISSADO, *Phys. Scripta* **T1** (1982) 110.
10. L. A. DISSADO and R. M. HILL, *Proc. R. Soc.* **A390** (1983) 131.
11. *Idem, J. Chem. Soc. Far. Trans. 2* **80** (1984) 291.
12. A. K. JONSCHER, *Coll. Polym. Sci.* **253** (1975) 231.
13. *Idem, Nature* **267** (1977) 673.
14. E. WARBURG, *Ann. Phys. Chem. (Neue Serie)* **67** (1899) 493.
15. K. S. COLE and R. H. COLE, *J. Chem. Phys.* **9** (1941) 341.
16. A. K. JONSCHER, *Thin Solid Films* **51** (1978) 133.
17. T. RAMDEEN, L. A. DISSADO and R. M. HILL, *J. Chem. Soc. Far. Trans. 1* **80** (1984) 325.
18. A. FAIRWEATHER and E. J. FROST, *Proc. IEE* **100** (1953) 15.
19. A. ISHIKAWA, T. HANAI and N. KOIZUMI, *Jpn. J. Appl. Phys.* **22** (1983) 942.
20. A. R. BRIGGS, private communication (1985).
21. J. R. MACDONALD and W. R. KENAN, Proceedings, of the Conference on Electrical Insulation and Dielectric Phenomena, Boston, 1980 (National Academy of Sciences, Washington DC, 1980) p. 3.
22. M. SHABLAKH, R. M. HILL and L. A. DISSADO, *J. Chem. Soc. Far. Trans. 2* **78** (1982) 525.
23. *Idem, ibid.* **78** (1982) 639.
24. M. SHABLAKH, L. A. DISSADO and R. M. HILL, *ibid.* **79** (1983) 369.
25. K. PATHMANATHAN, L. A. DISSADO and R. M. HILL, *J. Mater. Sci.* **20** (1985) 3716.

Received 14 December 1984
and accepted 15 January 1985